Thomas, N. M., Gray, R., Fry, C. H., Desplantez, T., Peters, N. S., Severs, N. J., ... Dupont, E. (2017). Functional consequences of co-expressing connexin40 or connexin45 with connexin43 on intercellular electrical coupling. *Biochemical and Biophysical Research Communications*, *483*(1), 191-196. https://doi.org/10.1016/j.bbrc.2016.12.169

Functional consequences of co-expressing connexin40 or connexin45 with connexin43 on intercellular electrical coupling

Neil M. Thomas, Rosaire Gray, Christopher H. Fry, Thomas Desplantez, Nicholas S. Petersa, Nicholas J. Severs, Kenneth T. Macleod, Emmanuel Dupont.

Highlights

•Cx40 and Cx45 are induced as a function of the dose of inducer.
•Endogenous Cx43 mRNA is reduced by induction of both Cx40 and Cx45.
•Cx43 protein is reduced by induction of Cx40 but not by induction of Cx45.
•Electrical coupling of monolayers is unchanged by induction of both Cx40 and Cx45.
•Cell morphology is altered by induction of Cx45.

Abstract

The functional characteristics of the co-expression of connexin43, connexin40, and connexin45 proteins in human myocardium are thought to play an important role in governing normal propagation of the cardiac electrical impulse and in generating the myocardial substrate for some arrhythmias and conduction disturbances.

A rat liver epithelial cell line, that endogenously expresses connexin43, was used to induce also expression of connexin40 or connexin45 after stable transfection using an inducible ecdysone system. Electrical coupling was estimated from measurement of the input resistance of transfected cells using an intracellular microelectrode to inject current and record changes to membrane potential.

However, varied expression of the transfected connexin40 or connexin45 did not change electrical coupling, although connexin43/40 co-expression led to better coupling than connexin43/45 co-expression. Quantification of endogenous connexin43 expression, at both mRNA and protein levels, showed that it was altered in a manner dependent on the transfected connexin isotype.

The data using rat liver epithelial cells indicate an increased electrical coupling upon expression of connexin40 and connexin43 but decreased coupling with connexin45 and connexin43 co-expression.

Keywords

Connexin; Gap junction; Heart; Inducible expression; Rat liver epithelial cells

1. Introduction

Gap junction channels directly link the internal environments of neighboring cardiac myocytes and therefore play a pivotal role in the direct cell-to-cell transfer of the electrical impulses which governs the coordinated contraction of the myocardium [9], [10] and [12]. Connexins are the principal components of gap junctions, and three members are expressed in cardiac myocytes: connexin43 (Cx43), connexin40 (Cx40) and connexin45 (Cx45). Disruption of gap junction distribution and remodeling of connexin expression are consistent features of human heart disease [29].

In the human heart, Cx43, Cx40 and Cx45 are co-expressed in distinctive combinations and relative quantities in different, functionally specialized subsets of myocytes [32]. While Cx43 is expressed in abundance throughout the atrial and ventricular myocardium, Cx40

and Cx45 display a greater degree of cell-type specificity. When individually expressed in transfected cells, gap junction channels composed of each connexin isotype display diverse functional properties [1], [15] and [25].

Because primary cultures of cardiomyocytes are not amenable to stable transfection, engineered rat liver epithelial (RLE) cells were used for this model. RLE cells were transfected to express variable levels of either Cx40 (ind40 cells) or Cx45 (ind45 cells) under the control of an exogenous inducible non-mammalian expression system (ecdysone system) against a background of endogenous Cx43 [8] and [17].

In previous studies, we found that altering connexin co-expression ratios in our cell lines directly changed the composition of gap junction channels at cell interfaces, and their cell-to-cell electrical conductance and dye permeability properties [8] and [17]. A noteworthy observation was that altered expression of the transfected connexins appeared to affect expression of the endogenous Cx43. In this study, we describe electrical coupling by macroscopic electrophysiological studies designed to evaluate further the functional consequences of altered connexin co-expression patterns as quantified by Western and Northern blot experiments.

2. Methods

2.1. Routine cell culture

RLE cells, engineered with the Ecdysone-Inducible Expression System (Invitrogen, CA, USA) to co-express Cx40, ind40 cells, or Cx45, ind45 cells, with endogenous Cx43, were cultured as described previously [8] and [17]. The mRNA expressed upon induction is a bi-cistronic mRNA, with an internal ribosome entry site between the connexin sequence and the antibiotic resistance. The maintenance medium contained 2 μM Ponasterone A (Pon-A) and 250 μg/ml hygromycinB to eliminate cells that lost inducibility. See Ref. [17] for a generic map of our constructs. To induce Cx40 or Cx45 expression, Pon-A was added to medium to a maximum concentration of 2 μM and incubated for ≥12 h in the absence of selection. Thereafter, cells were cultured in medium either with variable concentration of pon-A for ≥12 h.

2.2. Electrophysiological quantification of intracellular resistance

Electrical coupling of transfected cells was assessed through measurements of intracellular input resistance, Rinp, from the ratio of steady-state membrane potential deflection, Vss, in response to a current injection, I, i.e. Rinp = Vss/I [11], with adaption for an in vitro cell culture system Parental RLE cells form a uniform monolayer with a ‘cobblestone’ ap*p*earance. Thus *f*rom an injection site current wa*s expect*ed to disperse homogeneously in two dimensions. The transient phase of the voltage responses V, as a function of time, t, were always best fit with an exponential function, i.e. $V = A.(1-\exp(-t/\tau))$, where A is a constant and τ the characteristic time constant sug*g*esting uniform polarization of the cell area that was atta*i*nab*l*e to the *cu*rrent injec*t*ion. This enabled e*s*timation of changes to Rinp using a single microelectrode [11]. To preserve the intracellular milieu sharp micropipettes (20–40 MΩ) were used, fabricated from borosilicate glass capillaries (1.5 mm OD 0.86 mm ID; Harvard apparatus, MA, USA) with a horizontal pipette puller (Sutter Instruments, CA, USA), and back-filled with 3 M KCl. Once impaled, constant currents between 0.5 nA and 1.5 nA were injected into cells and perturbations of V recorded. Injected currents always ensured that Vss values never exceeded 100 mV,

and generally were less than 20 mV. Large trans-junctional voltage gradients alter the electrical properties of the junctions [2]. Electrical parameters were recorded using an Axoclamp-2B system in current-clamp mode, and pCLAMP software (Molecular Devices, CA, USA). All electrophysiological assessments were done at maximal induction (2 μM Pon-A) and at the steady state level of connexin expression after overnight incubation.

2.3. RNA extraction and Northern blotting

RNA extraction and Northern blotting were performed as described previously [4]. DNA probes were prepared using plasmid DNA used to engineer the ind40 and ind45 cell lines. Probes was used at a concentration of 2.5 ng/ml following random primer labeling with 32P-labeled dCTP radionucleotide (Roche, Basel, Switzerland). The same membranes were first hybridized for detection of the transfected connexin then re-hybridized for Cx43 detection. The membrane was re-hybridized for 18S rRNA detection: this is an accurate measure of total cellular RNA as a fixed proportion of ribosomal RNAs and related to cellular volume. Northern blots were quantified by scanning densitometry. Connexins signal was normalized to that obtained for 18S RNA [13]. A DNA 5′ End-labeling Kit (Boehringer-Mannheim, Ingelheim, Germany) and an oligonucleotide probe for 18S of known sequence Amersham Pharmacia Biotech, NJ, USA) were used according to the manufacturers' instructions.

2.4. Protein extraction and Western blotting

Western blotting and quantification were performed as described previously [14]. Primary antibodies used in Western blotting experiments were anti-Cx43 (MAB3067; Chemicon, CA, USA), anti-Cx40 (SC-20466; Santa Cruz, CA, USA) and anti-Cx45 (Q14E MAB19-11-5; in-house) [12] and [13]. Labeled connexin protein was visualized using alkaline phosphatase-conjugated secondary antibody and an NBT/BCIP Liquid Substrate System (Sigma, MO, USA). Bands were quantified by scanning densitometry using SigmaGel software (SPSS, IL, USA). The amounts of Cx40, Cx43 and Cx45 were compared to each other using lysates prepared from cell lines which express V5-tagged connexin proteins and an antibody calibration technique described previously [8] and [17]. Immunoreactions were normalized to total protein, which relates to cellular volume.

2.5. Statistical analysis

All statistical analyses were performed using GraphPad Prism 5 (GraphPad Software Inc., CA, USA). Data are expressed as mean ± standard error to the mean. Statistical relationships were evaluated by linear regression and judged as significant at $p < 0.05$. Curves were best-fit using an iterative least-squares method (KaleidaGraph, Synergy Inc).

3. Results

3.1. Electrophysiological assessment

Fig. 1a shows a representative tracing of the membrane potential (V) change in response to a current injection (I = 0.20 nA) through an intracellular microelectrode. The Em change was always fitted by a single exponential function, in this case with a time constant of 0.38 ms with a steady-state V (Vss) change of 8.1 mV (Rinp = 40.5 MΩ). The data from transfected RLE cell lines are shown in Fig. 1b and c, where input resistance (Rinp = Vss/I) is plotted against the time constant. The value of the time constant was indicative of

the total membrane capacitance of the preparation accessible to current from the intracellular microelectrode and therefore the amount of cell membrane. Each datum point represents the average of several current injections during impalement of a cell. The slope of the plot is thus an index of accessible membrane area per unit Rinp. Because Rinp is determined predominantly by intracellular resistance (in turn determined by intercellular electrical coupling by gap junctions), an increased slope indicates greater cell-to-cell coupling.

The upper plot in Fig. 1b shows results obtained for the ind40 cell line at maximal induction (24 impalements) and in the non-induced state (16 impalements). Plotting results for the induced and non-induced states together revealed that each fit yielded very similar linear regression lines. The slope of the regression line for maximal induction was 0.0109 ms/MΩ (r2 = 0.9800), and that for zero induction was 0.0111 ms/MΩ (r2 = 0.9066). This high degree of similarity indicated that alterations to Cx40:Cx43 co-expression ratios in ind40 cells had no effect on electrical coupling. The lower plot (1 c) shows results obtained for the ind45 cell line at maximal induction (22 impalements) and in the non-induced state (13 impalements). Again, the results obtained for the induced and non-induced states had linear fits with almost identical slopes i.e. maximal induction slope 0.00266 ms/MΩ (r2 = 0.5885), zero induction slope 0.00278 ms/MΩ (r2 = 0.8288). These data indicated that alterations to Cx45:Cx43 co-expression ratios in the ind45 cell line also had no effect on electrical coupling.

The spread of data obtained for each cell line suggested that the cell cultures consisted of functional clusters of cells of varying sizes. The exponential form of the voltage trace on current injection implies uniform polarization of each cluster, so that their diameter must be smaller than the space constant of the cell culture. The range of input resistances obtained for each cell line was very similar, and reached a maximum of approximately 500 MΩ. However, the slope obtained for the ind40 cell line (0.0110; r2 = 0.9342) was significantly steeper than that obtained for the ind45 cell line (0.0027; r2 = 0.7697). The ind40 cells displayed time constants to a maximum of ~4.5 ms, while the highest time constant was ~1.6 ms in ind45 cells. This indicated that cultures of ind40 cells formed functional clusters containing more cells, as assessed by electrical coupling, than preparations of ind45 cells.

3.2. Evaluation of connexin protein and transcript expression

Fig. 2 shows connexin transcript and protein expression in ind40 and ind45 cells cultured at incremental levels of induction.

To generate Northern and Western blots, cells were first maximally induced without antibiotic overnight in order to eliminate the remnants of hygromycin and then induced with Pon-A at the concentration indicated in the figure legend. Using this protocol, no mRNA or protein for Cx40 or Cx45 was detected without Pon-A in the medium and Cx43 mRNA and protein returned to control values.

The upper blots show Western blot and Northern analyses of transfected Cx40 and Cx45 expression in the ind40 and ind45 cell lines, respectively. Transcript and protein expression of the transfected connexins were observed to increase with induction in a dose-dependent manner in both cell lines. In ind40 cells Cx43 transcript and protein expression both decreased concomitant with induction. Cx43 transcript also decreased in

ind45 cell lines following induction but Cx43 protein appeared largely unchanged [8] and [17].

Quantitative analysis of Northern blot results suggested that Cx40 and Cx43 transcript expression in ind40 cells showed a moderate, negative correlation (r2 = 0.6469). Induction of Cx40 had an inhibitory effect on levels of Cx43 transcript. Cx45 ind45 cells also showed a moderate, negative correlation (r2 = 0.6355). Northern blot analyses using an indGFP displayed no significant alterations to Cx43 transcript expression indicating that this was a connexin-specific phenomenon.

Fig. 3 shows linear regression analysis of transcript expression data plotted against gap-junctional protein data in the ind40 and ind45 cell lines. Strong positive correlation between transfected Cx40 (a; r2 = 0.9224) and Cx45 (c; r2 = 0.9604) transcript with the amounts of their respective protein products. Endogenous Cx43 transcript and junctional protei displayed a strong positive correlation (r2 = 0.8591) in the ind40 cell line (b) but no significant correlation (r2 = 0.3150) was apparent between Cx43 transcript and protein in ind45 cells (d).

3.3. Cell morphology

Fig. 4 shows typical phase contrast micrographs of the transfected cell lines, and the parental RLE line as a control. In the induced state, ind45 (b) cells appeared larger and more elongated than ind40 (a) and control cells (c) which formed a uniform, cobblestone monolayer typical of RLE cells.

Upon removal of induction media, the morphology of both cell lines remained the same. The electrophysiological assessment in the non-induced state was done in the absence of Cx45 but presence of the morphological change which permitted direct comparison of the results. The approximately four-fold reduction of the slope of the time constant vs input resistance plots in Fig. 3b,C is consistent with a similar reduction of membrane surface area per unit area of culture. If following removal of induction, cells were also dissociated and re-seeded, ind45 (e) cell morphology revert to that of the ind40 (induced or not; a and d) or parental cell line (c and f). These changes were dependent on Cx45 expression only.

4. Discussion

RLE cells were selected because of their ease of transfection and their wild-type expression of Cx43 only. This has been shown by the voltage sensitivity and single channel conductance of gap junctions, as assessed by double patch clamp experiments that show the typical profile of gap junctions constituted by Cx43 only. Previously using these cell lines [8], we have shown that endogenous Cx43 and transfected Cx40 or Cx45 co-localize at cell-cell interfaces. The junctional and non-junctional fractions of connexins upon induction were quantified with biochemical methods using the differential TritonX-100 solubility. It was found that transfected RLE cell lines selectively co-localize specific quantities of different connexin isotypes at cell interfaces: equivalent amounts in the ind40 cell line (~50% Cx43/~50% Cx40) and equivalent but double the amounts in the ind45 cell line (~100% Cx43/~100% Cx45) at maximal induction. However, as shown here, an equivalent level of electrical coupling were maintained. Changes in the quantities of the less conductive Cx45 were accompanied by a change in cell morphology and increased size, the reason for this remains unclear.

Evidence for transregulation of connexin expression has been reported [20]. In the homozygous Cx40 knock-out mouse, deletion of Cx40 in the endothelium was accompanied by reduction of Cx43 protein expression [20]. It was shown that contrary to this study, deletion of one connexin in myocardium of transgenic mice was not accompanied by a compensatory change in expression of another connexin [18].

The cell monolayers were not electrically coupled throughout, but consisted of regions of cells of different sizes. This was deduced from the fact that the transient membrane potential responses from intracellular current injection were always best-fit with an exponential function implying uniform intracellular polarization. If the whole monolayer was electrically coupled a cable model would have been more appropriate to analyze the transient waveforms which demonstrates a non-exponential transient best-fit with a Bessel function [16]. Preliminary analyses with waveforms from induced and non-induced cells however never experienced a superior fit with a Bessel function.

Although ind40 and ind45 cell monolayers appeared to possess comparable resistance properties, ind40 cell clusters had a significantly higher capacitance than ind45 cells. This indicated that there were greater amounts of cell membrane in ind40 cell clusters than in a comparatively-sized clusters of ind45 cells composed of fewer but bigger cells.

The functional behavior of individual gap junction channels are well understood. On a macroscopic scale, the picture is less clear. Electrophysiological evaluation of the transfected RLE cells suggested a functional role for coordinated connexin co-expression patterns. Few studies have examined alterations to connexin co-expression ratios and electrical coupling, existing reports provide supportive findings. The A7r5 rat aortic smooth muscle cell line, expressing Cx40 and Cx43, maintains a uniform degree of electrical coupling in response to alterations to Cx40:Cx43 co-expression ratios; even when dye transfer is substantially altered [5].

As examined in detail [8], induction of Cx40 and Cx45, that are much less permeable to Lucifer Yellow than Cx43 [22], were accompanied by a loss of dye transfer measured using the scrape loading technique that was directly correlated with the level of induction of both Cx40 and Cx45. This loss of dye transfer directly correlated with the amounts of Cx43 in the ind40 cell line but not in the ind45 cells. As Cx40 and Cx43 are poorly compatible to form heterotypes [8] and [19] (hemichannels Cx40/Cx43) and since we did not observe a very large amount of heteromerisation (hemichannels containing both Cx43 and Cx40 are about12% of the junctional fraction) this indicated that most the dye transfer was mediated by homomer/homotypes constituted by Cx43. Therefore, the identical electrical coupling as measured here results from the replacement of Cx43 by an equivalent amount of Cx40 and the presence of some heteromers [8].

The reduction of dye transfer that correlated with the level of Cx45 induction even though junctional Cx43 was not reduced and no heteromerisation could be detected has led us to propose that Cx45 preferentially docks with Cx43 rather than with itself, thereby reducing dye transfer. The results of the present study are in accord with this proposal since at maximal induction, twice as much connexin is present in the junctions [9] but the observed coupling does not change as indicated by our electrophysiological assessment. The lack of difference in electrical coupling in the ind45 cells would therefore results from the formation of a large number of homomers/heterotypes at maximal induction with a single channel conductance of about ~60 pS which is equivalent to the coupling resulting from

the formation of half the number of homomers/homotypes constituted by Cx43 with a single channel conductance of about ~120 pS [14].

Electrical cell-to-cell conductance (Gj,0) displays a small, but non-significant increase in ind40 cells that fit well with the present study. Gj,0 was reduced by approximately 35% in ind45 cells [8]. Here we examined a large number of cells in a network constituted by multiple cell interfaces while in double patch-clamp experiments, single cell interfaces are examined. However, the reduction of Gj,0 still indicates that heterotypes constituted by C45 and Cx43 hemichannels are preferentially formed.

Our cell culture model displays compensatory change in the endogenous Cx43 expression but some conclusions can be drawn. An increase in Cx40 without change in Cx43 would have increased macroscopic electrical coupling. This explains that despite a smaller cell size in atrial tissues as compared to ventricular tissues that express the same amounts of Cx43, conduction velocities are equivalent in both tissues likely because Cx40 increases junctional conductance between atrial cells.

Conversely, expression of Cx45 in myocardial tissues would reduce electrical coupling since twice as much junctional connexin composed of Cx43 and Cx45 in equal amounts leads to the same electrical coupling as in the non-induced cells that express only Cx43. If Cx45 preferentially docks with Cx43, each Cx45 hemichannel docked with a Cx43 or Cx40 hemichannel will lower the conductance of the resulting junctional channel. This may be a mechanisms by which sino-atrial nodal cell that express mostly Cx45 can transmit the electrical impulses to the large sink of atrial tissues that express abundantly Cx43 and Cx40.

Our rationale was that results using two-dimensional arrays of cells were more representative of the function of multi-cellular networks such as cardiac tissues.

Funding sources
This study was supported by the British Heart Foundation (project grants PG/05/003 and PG/05/111) and by a PhD fellowship from the National Heart and Lung Institute.

Disclosures
None.

References

[1] F.F. Bukauskas, C. Elfgang, K. Willecke, et al.
Biophysical properties of gap junction channels formed by mouse connexin40 in induced pairs of transfected human HeLa cells
Biophys. J., 68 (1995), pp. 2289–2298

[2] F.F. Bukauskas, R. Weingart
Voltage-dependent gating of single gap junction channels in an insect cell line
Biophys. J., 67 (1994), pp. 613–625

[4] P. Chomczynski, N. Sacchi

The single-step method of RNA isolation by acid guanidinium thiocyanate-phenol-chloroform extraction: twenty-something years on
Nat. Protoc., 1 (2006), pp. 581–585

[5] G.T. Cottrell, J.M. Burt
Heterotypic gap junction channel formation between heteromeric and homomeric Cx40 and Cx43 connexons
Am. J. Physiol. Cell Physiol., 281 (2001), pp. C1559–C1567

[8] T. Desplantez, K. Grikscheit, N.M. Thomas, et al.
Relating specific connexin co-expression ratio to connexon composition and gap junction function
J. Mol. Cell. Cardiol., 89 (2015), pp. 195–202

[9] P.S. Dhillon, R.A. Chowdhury, P.M. Patel, et al.
Relationship between connexin expression and gap-junction resistivity in human atrial myocardium
Circ. Arrhythm. Electrophysiol., 7 (2014), pp. 321–329

[10] P.S. Dhillon, R. Gray, P. Kojodjojo, R. Jabr, et al.
Relationship between gap-junctional conductance and conduction velocity in mammalian myocardium
Circ. Arrhythm. Electrophysiol., 6 (2013), pp. 1208–1214

[11] M.H. Draper, S. Weidmann
Cardiac resting and action potentials recorded with an intracellular electrode
J. Physiol., 115 (1951), pp. 74–94

[12] E. Dupont, Y. Ko, S. Rothery, et al.
The gap-junctional protein connexin40 is elevated in patients susceptible to postoperative atrial fibrillation
Circulation, 103 (2001), pp. 842–849

[13] E. Dupont, T. Matsushita, R.A. Kaba, et al.
Altered connexin expression in human congestive heart failure
J. Mol. Cell. Cardiol., 33 (2001), pp. 359–371

[14] S. Elenes, A.D. Martinez, M. Delmar, et al.
Heterotypic docking of Cx43 and Cx45 connexons blocks fast voltage gating of Cx43
Biophys. J., 81 (2001), pp. 1406–1418

[15] C. Elfgang, R. Eckert, H. Lichtenberg-Frate, et al.
Specific permeability and selective formation of gap junction channels in connexin-transfected HeLa cells
J. Cell Biol., 129 (1995), pp. 805–817

[16] E.P. George
Resistance values in a syncytium
Aust. J. Exp. Biol. Med. Sci., 39 (1961), pp. 267–274

[17] K. Grikscheit, N. Thomas, A.F. Bruce, et al.
Coexpression of connexin 45 with connexin 43 decreases gap junction size
Cell Commun. Adhes., 15 (2008), pp. 185–193

[18] D. Gros, L. Dupays, S. Alcolea, et al.
Genetically modified mice: tools to decode the functions of connexins in the heart-new models for cardiovascular research
Cardiovasc. Res., 62 (2004), pp. 299–308

[19] D.B. Gros, H.J. Jongsma
Connexins in mammalian heart function
Bioessays, 18 (1996), pp. 719–730

[20] B.E. Isakson, D.N. Damon, K.H. Day, et al.
Connexin40 and connexin43 in mouse aortic endothe*lium:* evidence for coordinated regulation
Am. J. Physiol. Heart Circ. Physiol., 290 (2006), pp. H1199–H1205

[22] G. Kanaporis, P.R. Brink, V. Valiunas
Gap junction permeability: selectivity for anionic and cati*onic p*robes
Am. J. Physiol. Cell Physiol., 300 (2011), pp. C600–C609

[25] A.P. Moreno, M.B. Rook, G.I. Fishman, et al.
Gap junction channels: distinct voltage-sensitive and -insensitive conductance states
Biophys. J., 67 (1994), pp. 113–119

[29] N.J. Severs, E. Dupont, N. Thomas, et al.
Alterations in *cardi*ac connexin expression in cardiomyopathies
Adv. Cardiol., 42 (2006), pp. 228–242

[32] C. Vozzi, E. Dupont, S.R. Coppen, et al.
Chamber-related differences in connex*in exp*ression in the human heart
J. Mol. Cell. Cardiol., 31 (1999), pp. 991–1003

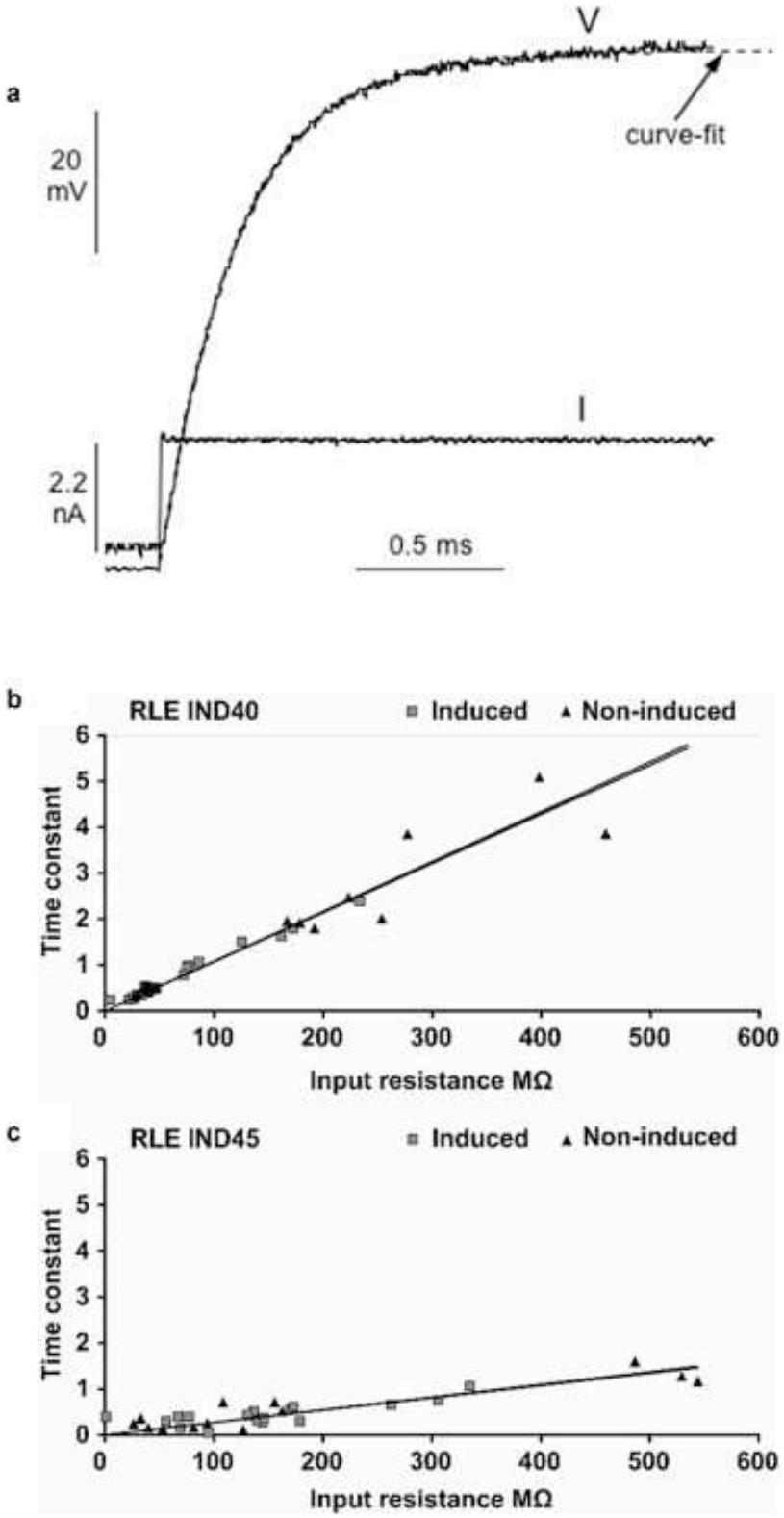

Figure 1. Electrical coupling in RLE IND40 and IND45 cells. a: Recording from RLE ind40 cells showing the membrane potential response (V) upon injection of a current (I) with an intracellular electrode. b and c: Time constant of V-response as a function of input resistance (Rinp, MΩ), in ind40 and ind45 cells at zero induction (black triangles) and maximal induction (grey squares). The r2 values of the linear fits are given in the Result section (3.1 Electrophysiological assessment).

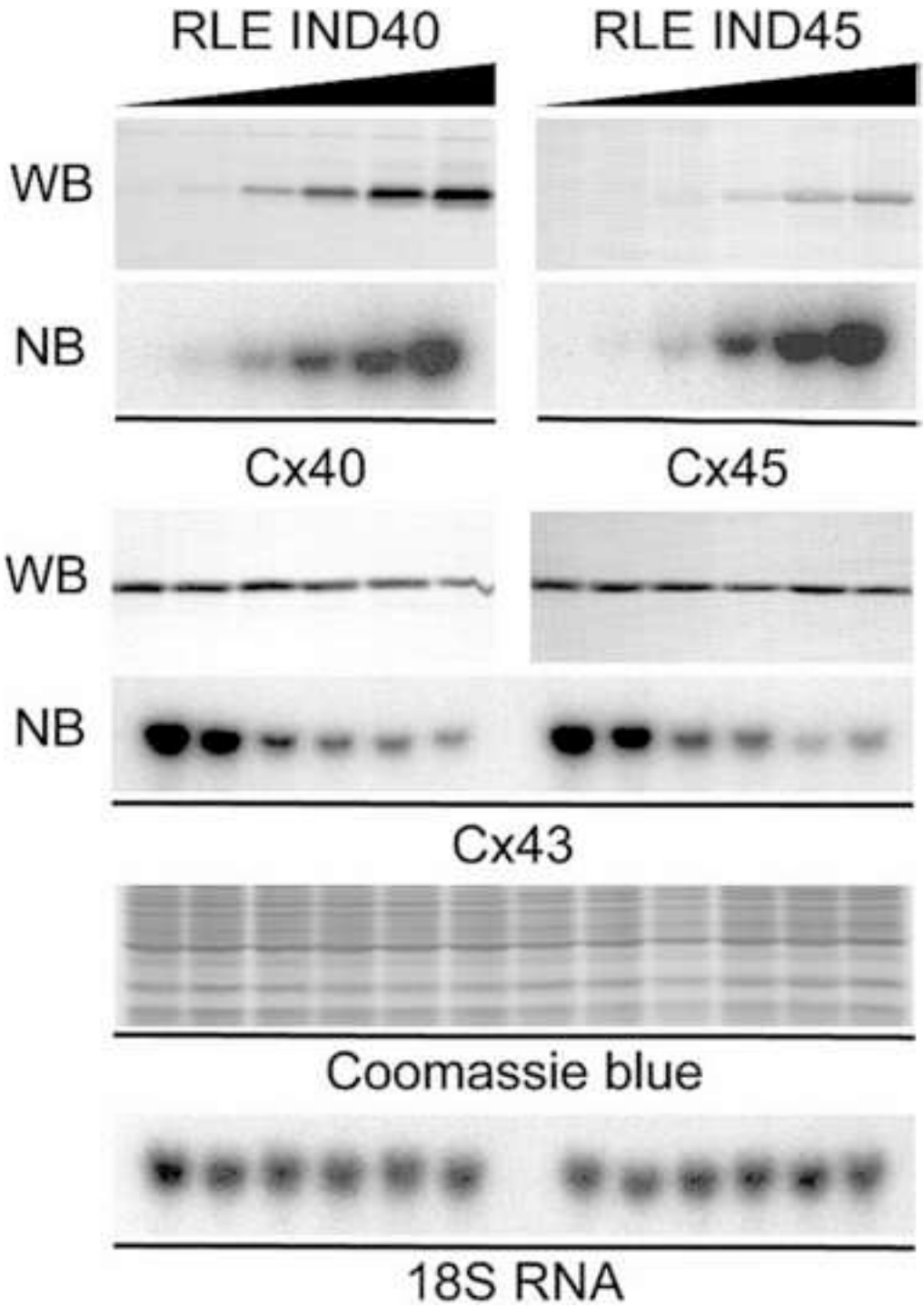

Fig. 2. Northern and Western blot analyses of connexin co-expression in the RLE IND40 and IND45 cell lines. Northern (NB) and Western (WB) blots depict transcript and protein expression of transfected Cx40 and Cx45, and endogenous Cx43 expression in ind40 and ind45 cells. Connexin transcript signal was normalized to signal for 18S ribosomal and protein signal was normalized to total protein in Western blots. Both normalization procedures relate to cellular volume. The coomassie blue gel is presented here to show equivalent loading of the gels used for western blots. Progressively higher levels of induction are illustrated by black arrows (0, 0.1, 0.25, 0.5, 1 and 2 μM Pon-A).

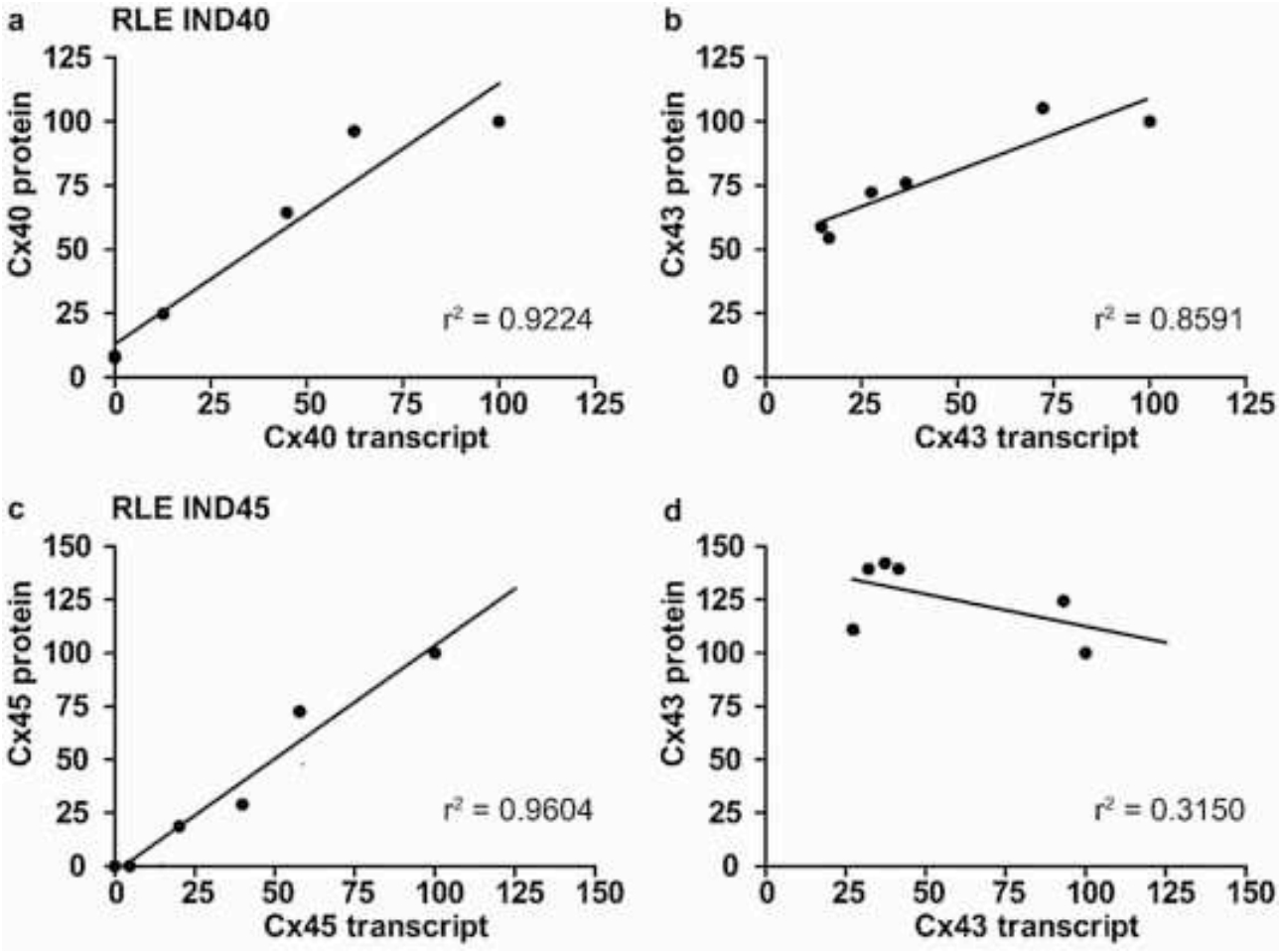

Fig. 3. Concordance between connexin transcript expression and connexin protein localization in gap junctions. (a)–(d) linear regression analyses performed to determine if connexin abundance in gap junctions is regulated by transcription in transfected RLE. All expression values were standardized to 100. For transfected connexins, 100 represents expression at maximal induction. For endogenous Cx43, 100 represents wild type expression at zero induction (Western blot n = 3 vs. Northern blot n = 3).

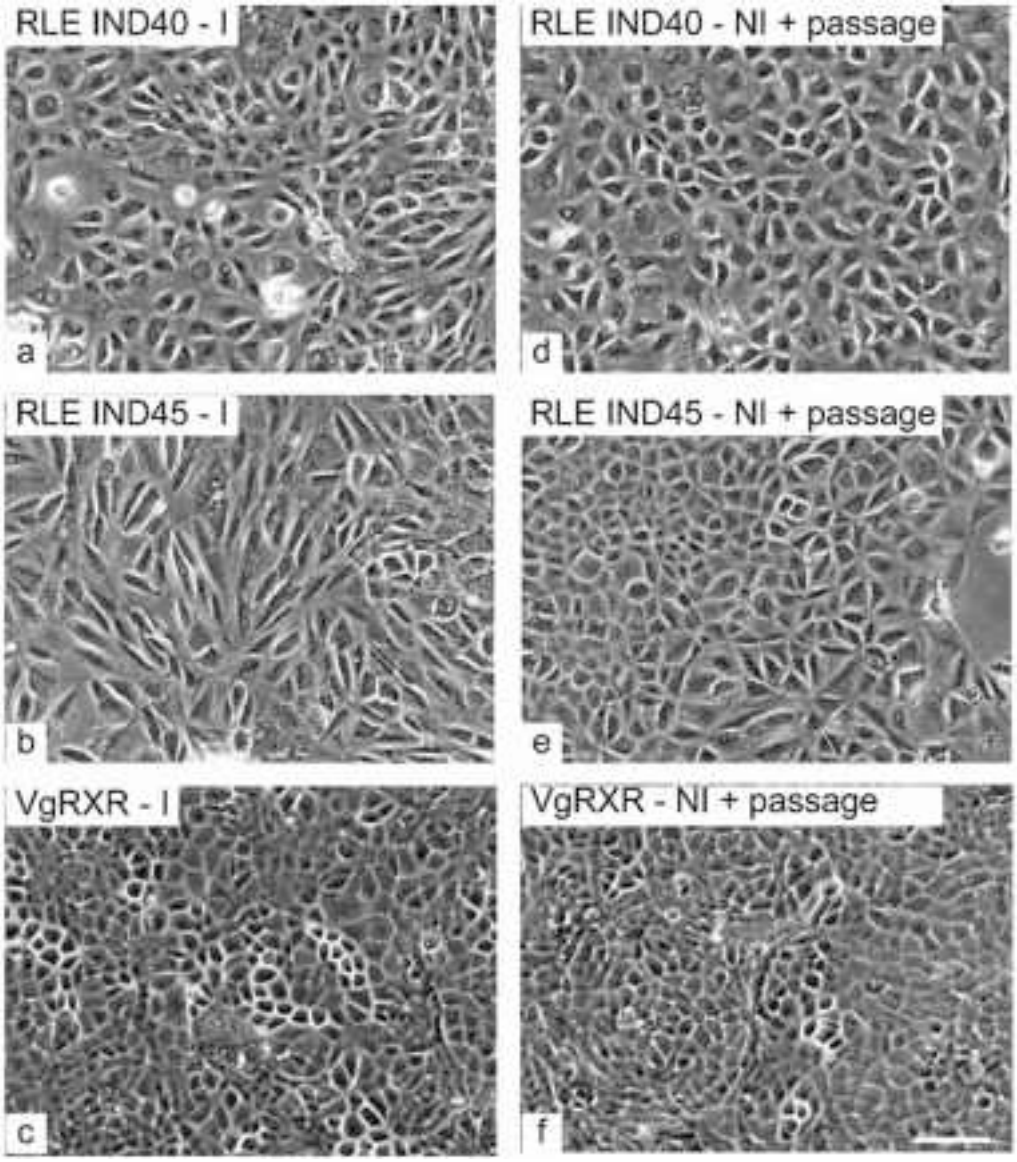

Fig. 4. Cx40 and Cx45 expression alters morphology of transfected RLE cell lines. (a)–(c) show phase contrast micrographs of the morphological response of ind40, ind45 and control VgRXR cells to maximal induction. (d)–(f) show the morphology of the same cells without induction but after dissociation and re-seeding. I: induced; NI: non-induced. Bar: 50 μm.